



DOI:10.22144/ctujoisd.2025.036

Study on catalytic activity of bimetallic CuZn-ZIFs for Rhodamine B decomposition in the presence of potassium peroxymonosulfate

Tran Ba Huy¹, Nguyen Dinh Thanh¹, Nguyen Minh Nhut¹, Ho Ngoc Tri Tan¹,
and Dang Huynh Giao^{1,2*}

¹College of Engineering, Can Tho University, Viet Nam

²Applied Chemical Engineering Laboratory, College of Engineering, Can Tho University, Viet Nam

*Corresponding author (dhgiao@ctu.edu.vn)

Article info.

Received 30 Jun 2024

Revised 27 Jul 2024

Accepted 13 Jan 2025

Keywords

Catalysis, CuZn-ZIFs,
Decomposition, Potassium
peroxymonosulfate,
Rhodamine B

ABSTRACT

Rhodamine B (RhB) is a highly toxic dye that poses significant health risks. In this study, CuZn-ZIFs was synthesized and analyzed by various techniques such as Powder X-ray diffraction (PXRD), Fourier-transform infrared spectroscopy (FT-IR), Thermogravimetric analysis (TGA), Scanning electron microscopy (SEM), energy-dispersive X-ray spectrometer (EDS) and Brunauer–Emmett–Teller (BET). In clearly defined technical parameters, CuZn-ZIFs exhibited a notable heat resistance up to 600°C and featured a distinct polygonal structure. Furthermore, an assessment revealed a Specific Surface Area of 1242.7 m²·g⁻¹, accompanied by a pore volume of 0.47 cm³·g⁻¹, a pore size measuring 11.53 Å, and an average particle size of 28.67 nm. Not only that, it was found to be effective in promoting the oxidation of peroxymonosulfate (PMS) for RhB treatment. The results showed that over 90% of RhB concentration 40 mg·L⁻¹ was degraded within 50 minutes in the presence of PMS and 0.15 g·L⁻¹ of CuZn-ZIFs catalyst at room temperature. Additionally, the catalyst demonstrated remarkable reusability, maintaining high removal efficiency after five cycles. It indicated that this material has great potential as an effective heterogeneous catalyst for removing toxic dyes from aqueous solutions.

1. INTRODUCTION

Environmental pollution has been a major concern for a long time, especially water pollution caused by toxic chemicals, which has reached alarming levels. The extent of pollution in wastewater is mainly dependent on the types of chemicals, auxiliary substances, dyes used, as well as the level of technology used, whether it is outdated, average, advanced, or modern (Carmen & Daniela, 2012). Numerous studies have demonstrated that even mild contamination of organic dyes can lead to vomiting and poisoning (Samuel et al., 2021). Over time, the

accumulation of these dyes in the body can even lead to cancer. Skin exposure to these dyes can cause itching and allergic reactions. Inhaling these dyes can result in symptoms such as chest tightness, difficulty breathing, itchy neck, coughing, and sore throat (You et al., 2018). Annually, approximately 70 million tons of dyes are produced. These dyes are often organic compounds that are difficult to decompose in natural environments due to their stable structures (Chandanshive et al., 2020). Therefore, scientists are always faced with the challenge of finding new materials and methods to treat organic dyes.

Among the organic dyes, Rhodamine B (RhB), a red cationic dye, is widely used in biology as a fluorescent dye. It is often combined with auramine O to create auramine-rhodamine stain, which are used to demonstrate acid-degrading organisms, especially *Mycobacterium*. RhB dye is highly durable because its structural formula contains many benzene rings and strong naphthalene rings. Because it includes many aromatic rings, it is also a direct agent that can cause hazards to human health, such as cancer and damage to the nervous system (Sa et al., 2016). Therefore, many methods have been applied to remove RhB including adsorption (Wang & Zhu, 2007), photocatalysis (Yusufl et al., 2022), ultrasound (Zhang & Liu, 2020), oxidation (Fatima & Sultana, 2009) and microwaves (Lee et al., 2012). Most methods still have drawbacks, such as high costs, inefficiency, or generation of toxic byproducts (Asad et al., 2009). Typically, the adsorption method cannot completely remove the benzene and naphthalene rings in the structure of RhB because the nature of adsorption is to collect dye molecules in the porous structure of the material (Wang & Zhu, 2007). The photocatalytic method requires a long irradiation time but cannot completely decompose RhB (Lachheb et al., 2002). Ultrasonic and microwave methods often require harsh reaction conditions and higher costs. Compared to the above methods, oxidation offers many advantages in decomposing RhB due to the mechanism of bond breaking involving benzene and naphthalene rings in the chemical structure to create benign, less toxic products.

Metal-organic frameworks (MOFs) are a type of porous material with a crystalline structure composed of metal ions connected by organic molecules. MOFs have many unique properties, including thermal stability, high chemical stability, large specific surface area, and flexible structural framework. Due to these properties, MOFs have the potential for various applications, such as gas storage and separation, adsorption, sensing, and drug delivery (Dey et al., 2014). In particular, Zeolitic imidazolate frameworks (ZIFs) are a subclass of the group of MOFs, almost inherit the characteristics of MOFs (Zhong et al., 2018), have still a wide range of applications in various fields such as adsorption (Wang & Zhu, 2007), gas storage (Assfour et al., 2011), drug delivery (Wang et al., 2012) and particularly in the field of catalysis (Nagarjun & Dhakshinamoorthy, 2019). Recent studies have demonstrated that doped materials have improved performance, properties, structure, and

catalytic activity compared to conventional ZIFs materials (Budi et al., 2021). Herein, a bimetallic material, CuZn-ZIFs, was synthesized by doping Cu^{2+} ions into the ZIF-8 material framework using solvothermal synthesis (Schejn et al., 2015), hydrothermal, ultrasound (Zhang & Liu, 2020), microwave (Awadallah et al., 2019), and mechanical (Dai et al., 2019). The Cu^{2+} ion was chosen because it has an ionic radius close to that of Zn^{2+} in the tetrahedral arrangement (0.73Å and 0.74Å). CuZn-ZIFs are currently of interest and application to many scientists in the fields of adsorption (Nagarjun & Dhakshinamoorthy, 2019), catalysis (Dai et al., 2019), and antibacterial (Kumar et al., 2020). For example, Awadallah and his colleagues (2019) synthesized CuZn-ZIFs to study the adsorption and separation of propane, propylene, isobutane, and *n*-butane gas at 25°C. The research team conducted a study on the adsorption of CuZn-ZIFs on different types of gases, such as N_2 , CH_4 , and CO_2 . The results showed that the adsorption capacity of CuZn-ZIFs was higher than that of the precursor ZIF-8 (Awadallah et al., 2019). In addition, the material's high adsorption potential was appreciated for its successful treatment of the antibiotic doxycycline hydrochloride (DCH). The maximum adsorption capacity of CuZn-ZIFs was $379.2 \text{ mg} \cdot \text{g}^{-1}$, which was higher than the available ZIF-8 ($239.2 \text{ mg} \cdot \text{g}^{-1}$) (Zhang and Liu, 2020). Besides, CuZn-ZIFs are a type of catalyst that is very effective in various chemical reactions. Li and his colleagues discovered that they work especially well in the photocatalytic decomposition of methylene blue (MB) under light irradiation (Li et al., 2013). In addition to this, CuZn-ZIFs are also used to catalyze other chemical reactions, such as Friedlander and Combes condensation reactions (Schejn et al., 2015). Dai also reported that the dehydrogenation reaction of PhMe_2SiH and *n*-butanol occurred in the presence of CuZn-ZIFs catalyst (Dai et al., 2019). Moreover, Kumar et al. (2020) investigated the production of medical masks composed of copper@ZIF-8 core-shell nanowires (Cu@ZIF-8 NWs) to combat *Streptococcus mutans* and *Escherichia coli*.

Diverse methods are employed for RhB treatment, such as adsorption and decomposition, but their effectiveness varies. For instance, Ren et al. (2022) studied Fe-MOF materials and found that the adsorption of RhB was effective, with a capacity of $135 \text{ mg} \cdot \text{g}^{-1}$ in 4 hours. Similarly, Song et al. (2022) used powdered activated carbon to adsorb RhB at a

capacity of $28.6 \text{ mg} \cdot \text{g}^{-1}$ with a concentration of RhB $40 \text{ mg} \cdot \text{L}^{-1}$.

Past research has indicated that CuZn-ZIFs can be synthesized in various ways and have applications in different fields, particularly in the treatment of textile wastewater, making it a promising material for environmental remediation. Some studies have reported the use of ZIFs materials to adsorb RhB dye. Nevertheless, this approach has the drawback of not completely addressing pollutants. Consequently, the objective of this study is to address RhB dye through the catalytic decomposition method using the catalytic material CuZn-ZIFs and the oxidizing agent PMS, offering a new and more comprehensive treatment approach.

2. MATERIALS AND METHOD

2.1. Materials

The chemicals used in this study included 2-Methylimidazole ($\text{C}_4\text{H}_6\text{N}_2$, 99%) originated from Acros, USA. Methanol ($\text{C}_2\text{H}_5\text{OH}$, 99.5%), Zinc nitrate hexahydrate ($\text{Zn}(\text{NO}_3)_2 \cdot 6\text{H}_2\text{O}$, 99%), Copper (II) nitrate trihydrate ($\text{Cu}(\text{NO}_3)_2 \cdot 3\text{H}_2\text{O}$, 99%), Potassium peroxymonosulfate ($2\text{KHSO}_5 \cdot \text{KHSO}_4 \cdot \text{K}_2\text{SO}_4$, 47%) originated from Sigma - Aldrich, USA and Rhodamine B ($\text{C}_{28}\text{H}_{31}\text{N}_2\text{O}_3\text{Cl}$, 99%) was purchased from Xilong Chemical Co., Ltd, China. All chemicals in this research were used directly, without any additional purification.

2.2. Method

2.2.1. Synthesis of CuZn-ZIFs

CuZn-ZIFs was synthesized by the combined solvent-ultrasound method based on the research of Zhang and Liu (2020). In general, 1.22 g of $\text{Zn}(\text{NO}_3)_2 \cdot 6\text{H}_2\text{O}$ and 0.4 g of $\text{Cu}(\text{NO}_3)_2 \cdot 3\text{H}_2\text{O}$ were dissolved separately in 10 mL of methanol. Then, the zinc salt solution was slowly added to the copper salt solution and stirred for 15 minutes. The mixture was then slowly introduced into a beaker containing 2.23 g of 2-methylimidazole (2-MIm) ligand dissolved in 10 mL of MeOH. The metal salt mixture was gradually added to the 2 MIm solution by a burette and the mixture was stirred at room temperature for 10 min. The mixture was then cleaned by ultrasound for 15 min at 60°C . To facilitate the formation of material crystals, the sample was left to stand for 24 hours. Then, the precipitate was obtained by centrifugation and washed with MeOH several times to remove all

remaining substances. Finally, CuZn-ZIFs was dried at 60°C for 24 h.

2.2.2. Characterization of CuZn-ZIFs

The CuZn-ZIFs characteristic was analyzed by using several techniques. The powder X-ray diffraction (PXRD) analysis was employed to reveal the crystal structure of samples with a $\text{Cu K}\alpha$ ($\lambda = 1.5406 \text{ \AA}$) radiation source on D8 Advance-Brucker powder diffraction spectrometer. The Fourier-transform infrared spectroscopy (FT-IR) was recorded to determine the samples' functional group links. Energy dispersive X-ray spectroscopy (EDX) was applied to detect the chemical elements present in CuZn-ZIFs. The internal morphology and structural characteristics were observed by the scanning electron microscopy (SEM, Hitachi S4800). Additionally, thermogravimetric analysis (TGA) was performed on a Setaram Labsys Evo instrument in N_2 gas from a temperature of 900°C with a heating rate of $10^\circ\text{C} \cdot \text{min}^{-1}$ and the specific surface areas of CuZn-ZIFs were determined based on their N_2 adsorption-desorption isotherms and the Brunauer-Emmett-Teller (BET) model.

2.2.3. Catalytic degradation experiment

The activity investigation experiment was conducted by dispersing an amount of CuZn-ZIFs material and PMS oxidant in a ratio (1:4) in 20 mL of RhB solution with a determined concentration, the mixture was stirred magnetically at a speed of 400 rpm^{-1} until the end of the survey. Separate the material and RhB solution after the reaction by filtration and centrifugation. The residual RhB content was measured by a UV-Vis spectrophotometer at the maximum wavelength of RhB 553 nm (Figure 1). The results were compared with the standard curve to calculate RhB removal efficiency. RhB removal efficiency was calculated according to the formula as follows.

$$H\% = \left(\frac{C_0 - C_e}{C_0} \right) \times 100\%$$

In there:

H%: RhB removal efficiency (%)

C_0 : initial RhB concentration ($\text{mg} \cdot \text{L}^{-1}$)

C_e : remaining RhB concentration ($\text{mg} \cdot \text{L}^{-1}$)

Factors affecting the RhB treatment process were investigated, including the initial concentration of RhB, dosage of CuZn-ZIFs material, ratio of PMS oxidant to material dosage, temperature, and reaction time.

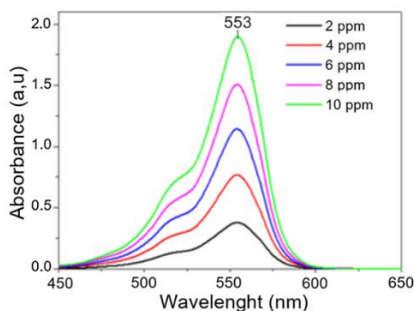


Figure 1. UV-vis of Rhodamine B at different concentrations

2.2.4. Reusability experiments

The process of recovering and evaluating the reusability of CuZn-ZIFs has been studied for its performance in catalytic degradation of RhB under optimal conditions. After treatment, the mixture was centrifuged to recover the catalyst. CuZn-ZIFs was then washed several times with methanol and activated at 60°C for 24 hours. Next, the above CuZn-ZIFs was evaluated for activity like previous experiments through the UV-Vis method and were re-analyzed to assess their structural stability by PXRD and FT-IR spectroscopy.

3. RESULTS AND DISCUSSION

3.1. Characterization of CuZn-ZIFs

PXRD analysis determined the structural intensity of CuZn-ZIFs. The characteristic peaks in the

PXRD diagram of CuZn-ZIFs and Zn-ZIFs were shown in Figure 2(a) showed that appearing at the 2θ angle position are 7.3°, 10.3°, 12.7°, 14.7°, 16.4°, and 18° with faces (011), (022), (112), (022), (013) and (222) matched previous studies (Zhang & Liu, 2020), (Thanh et al., 2023). Doping Cu into Zn-ZIFs did not change its original structure much due to the similar ionic radii of Cu²⁺ and Zn²⁺. This confirmed the successful synthesis of CuZn-ZIFs in MeOH with ultrasonic waves at room temperature, forming crystals with good structure and high crystallinity.

Determining crystallite size from PXRD data using the Scherrer equation: the Scherrer equation, expressed as:

$$D = \frac{K\lambda}{\beta \cos\theta}$$

where D is the average crystallite size in nm, K is the Scherrer constant, λ is the X-ray wavelength, CuKα = 0.15406Å, β is the line broadening at FWHM in radians, and θ is the Bragg angles. The average size of the crystal grains in BCMF was determined to be 28.67 nm using the Scherrer equation, considering the strongest diffraction peak. The Scherrer constant used was 0.94, and the full width at half maximum (FWHM) of the peak was taken into account. Thus, the measured diameter for BCMF was 28.67 nm.

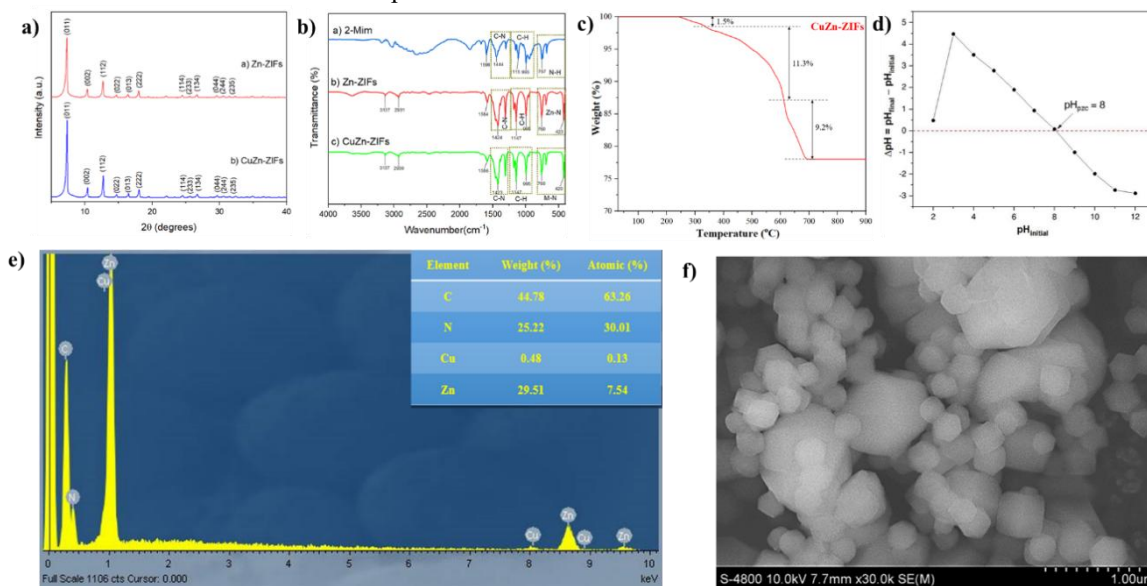


Figure 2. PXRD pattern of CuZn-ZIFs, Zn-ZIFs (a), FT-IR spectrum of CuZn-ZIFs, Zn-ZIFs, 2-MIm (b), TGA curve of CuZn-ZIFs (c), pHpzc of CuZn-ZIFs (d), EDX spectra of CuZn-ZIFs (e), and SEM image of CuZn-ZIFs (f)

CuZn-ZIFs was analyzed using infrared spectroscopy to identify functional groups. The results were compared with Zn-ZIFs spectrum and 2-methylimidazole ligand for convenience comparison, as shown in Figure 2(b). Characteristic peaks in the FT-IR results showed similarities between Zn-ZIFs and CuZn-ZIFs. Zn-ZIFs had peaks at 421.86 cm^{-1} , 685 cm^{-1} , 759.83 cm^{-1} , indicating Zn-N bonds. CuZn-ZIFs had additional peaks at 422.12 cm^{-1} , 694.18 cm^{-1} , and 760.09 cm^{-1} in addition. Metallic frameworks with C-H bonds were observed in both materials. The presence of 2-methylimidazole (2-Mim) with a signal range extending from $3200\text{--}2200\text{ cm}^{-1}$ represents the characteristic H-N-H bond in the material structure. Notably, the above results are almost unchanged from the previous reports of (Thanh et al., 2023). However, further analysis using energy dispersive X-ray spectroscopy (EDX) is necessary to determine element composition and content. Thermal stability is crucial for solid materials. The thermal stability of CuZn-ZIFs was analyzed using TGA at a heating rate of $10^\circ\text{C}\cdot\text{min}^{-1}$. The TGA analysis showed a decreasing curve, indicating material volume reduction. The temperature range of $250\text{--}400^\circ\text{C}$ showed a decrease, possibly due to a mixture of air adsorbed and methanol. The mass loss occurred at $450\text{--}700^\circ\text{C}$ due to the decomposition of the 2-Mim ligand in the CuZn-ZIFs framework. The remaining mass consisted of Cu and Zn oxides. The pH at which the surface of a material has a neutral charge is known as the point of zero charge (pHpzc). The pHpzc of CuZn-ZIFs was determined to be approximately 8, as shown in Figure 2(d). This value was similar to the pHpzc of ZIF-8 (9.5) and ZIF-67 (8.7). The pHpzc of the material provided insight into the surface charge of the material under different pH conditions. When the pH of the solution was lower than the pHpzc, the surface of CuZn-ZIFs could have a positive charge. Conversely, if the pH of the solution was greater than 8, CuZn-ZIFs would carry a negative charge on its surface. The EDX analysis of the CuZn-ZIFs sample in Figure 2(e) revealed the presence of elemental composition, including C, N, H, Zn, and Cu. The spectrum confirmed the successful synthesis of CuZn-ZIFs with Cu doping in the Zn-ZIFs structure. Zn and Cu act as metal nodes connected to the N position on 2-MIm. The EDX results also showed mass and element percentages, with Cu accounting for only 0.48% due to random doping without specific rules. The CuZn-ZIFs continued to be examined for surface structure characteristics by conducting SEM imaging with different magnifications, as shown in

Figure 2(f). Results from SEM images showed that the synthesized material has a polygonal cubic structure and is almost the same structure as the synthesized Zn-ZIFs. However, the particle sizes were relatively uneven, showing that the structure of the CuZn-ZIFs was consistent with previous studies. At the same time, the figure showed that the synthesized materials were completely identical because the Cu metal coordination did not hinder the initial crystal formation of Zn-ZIFs. This study employed the BET method to calculate the specific surface area. The specific surface area was determined to be $1242.7\text{ m}^2\cdot\text{g}^{-1}$, with a pore volume of $0.47\text{ cm}^3\cdot\text{g}^{-1}$ and a pore size of 11.53 \AA . Notably, the BET surface area reported in this study was lower than that reported by Zhang and Liu (2020) whose value was $1339.7\text{ m}^2\cdot\text{g}^{-1}$. However, the value exceeds that reported by Thanh et al. (2023), which was $1004\text{ m}^2\cdot\text{g}^{-1}$. In addition, the three studies' pore volume and size remained relatively unchanged. Specifically, in Zhang and Liu's study, the pore volume and pore size were reported as $0.53\text{ cm}^3\cdot\text{g}^{-1}$ and 13.85 \AA . As for the study of Thanh et al. (2023), the pore volume and pore size were reported as $0.46\text{ cm}^3\cdot\text{g}^{-1}$ and 16.7 \AA , respectively.

In brief, the structural and morphological features of the CuZn-ZIFs materials examined in this study, when compared to those in previous research, confirm their successful synthesis. Moreover, the results obtained were nearly identical to those of prior studies.

3.2. RhB catalytic decomposition

CuZn-ZIFs was produced in MeOH by the solvent heating method combined with ultrasound. After researching and proving the structural properties, research was conducted on the catalytic activity of the material for RhB treatment in the presence of potassium peroxymonosulphate. RhB solution, CuZn-ZIFs catalyst, and PMS are all part of the reaction system. The main mechanism for RhB removal depends on the hydroxyl radical ($\cdot\text{OH}$), which is mainly generated by CuZn-ZIFs catalytic PMS. The hydroxyl free radical is recognized as a powerful core for processing complex chemicals. The factors investigated include pH, the initial concentration of RhB, catalysis dosage of CuZn-ZIFs material, dosage ratio of (CuZn-ZIFs: PMS), temperature, and reaction time were all examined.

3.2.1. Influence of pH

The catalytic activity of the material was evaluated through the RhB decomposition reaction in the

presence of PMS. CuZn-ZIFs played a catalytic to stimulate the decomposition of PMS to create free radicals hydroxyl ($\cdot\text{OH}$). These free radicals were the main agents that attacked and decomposed dye molecules. This process is similar to the Fenton process; however, the catalyst used is heterogeneous and has the potential to be recovered and reused. The pH ranges investigated were from 3 to 8 with fixed factors of catalyst dosage of $0.15 \text{ g}\cdot\text{L}^{-1}$, PMS: CuZn-ZIFs (1:4), room temperature, time of 60 minutes, and initial Rhodamine B concentration is $40 \text{ mg}\cdot\text{L}^{-1}$. The results were shown in Figure 3. When the pH increases from 3 to 8, the RhB decomposition efficiency decreases. Specifically, when pH increases from 3–8, the efficiency decreases from 100% to 49%. This proved that pH decomposed PMS in a basic environment, thereby limiting the formation of free radicals necessary for the catalytic process. Besides, because the CuZn-ZIFs surface had a positive charge when the solution pH increased, negative ions interacted with the material surface, leading to a negatively charged material surface, reducing the interaction between PMS and thus reducing the free radicals produced.

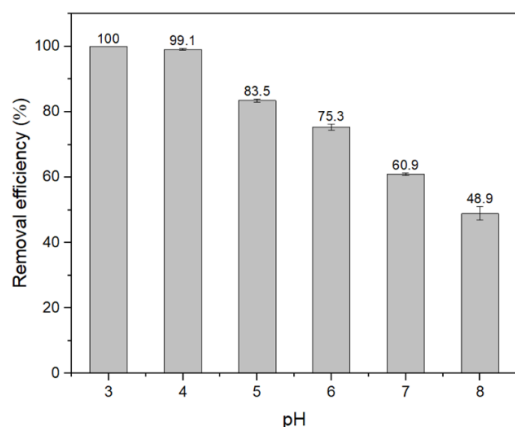


Figure 3. RhB removal efficiency of CuZn-ZIFs/PMS system with different pH

Experimental conditions: RhB concentration of $40 \text{ mg}\cdot\text{L}^{-1}$, CuZn-ZIFs dosage of $0.15 \text{ g}\cdot\text{L}^{-1}$, CuZn-ZIFs:PMS ratio (1:4), room temperature and reaction time of 60 min.

3.2.2. Influence of initial RhB concentration

In reality, the concentration of dyes in industrial wastewater is variable and cannot be regulated. Therefore, the initial RhB concentration is the factor investigated to consider the catalytic ability of CuZn-ZIFs in the presence of PMS oxidant in decomposing RhB in environments with high concentrations. The difference was varied from 10-

$50 \text{ mg}\cdot\text{L}^{-1}$ with fixed factors including RhB solution with pH 4, the amount of CuZn-ZIFs was $0.15 \text{ g}\cdot\text{L}^{-1}$, the ratio of catalyst dosage to PMS oxidant was 1:4, the reaction was carried out at room temperature for 60 minutes. The results are presented in Figure 4. According to experiments, with RhB concentration from 10 to $50 \text{ mg}\cdot\text{L}^{-1}$, the RhB removal efficiency was as high as 99 - 100%, but when continuing to increase the RhB concentration from $50 \text{ mg}\cdot\text{L}^{-1}$, the efficiency gradually diminished. It could be explained that when fixing a reaction time, hydroxyl radicals were produced in the same amount based on the ratio between catalyst and PMS, so when increasing RhB concentration, the possibility of contact between the molecules increased. Hydroxyl free radicals and active centers on the material decreased; conversely, the lower the concentration, the $\cdot\text{OH}$ radicals easily broke the stable bonds in the drug molecule in the same fixed time.

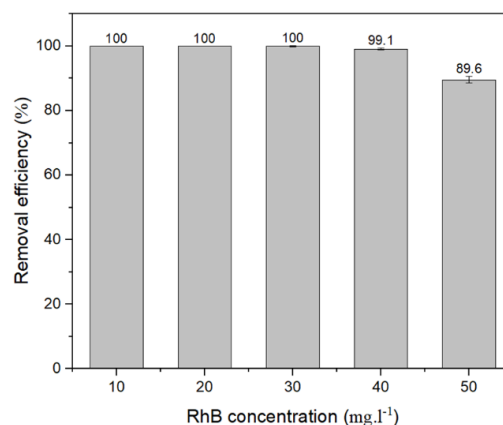


Figure 4. RhB removal efficiency of CuZn-ZIFs/PMS system with different initial RhB concentrations

Experimental conditions: CuZn-ZIFs dosage of $0.15 \text{ g}\cdot\text{L}^{-1}$, CuZn-ZIFs:PMS ratio (1:4), pH = 4, room temperature and reaction time of 60 min.

3.2.3. Influence of catalyst dosage

The CuZn-ZIFs content was a crucial factor in the reaction system because it catalyzed PMS to produce $\cdot\text{OH}$ radical and $\text{SO}_4^{\cdot-}$ sulfate radical - the agent that directly removes RhB. To determine the role of the catalyst, experiments were designed with CuZn-ZIFs catalysis dosage from 0 to $0.25 \text{ g}\cdot\text{L}^{-1}$. The fixed factor includes RhB concentration of $40 \text{ mg}\cdot\text{L}^{-1}$ with pH 4, the ratio of catalyst to PMS was 1:4, and the reaction was performed at room temperature for 60 minutes. The results are

presented in Figure 5. Survey results showed that when only PMS and RhB are present, the removal efficiency is very low (about 14.9%). The effective removal of RhB in the absence of CuZn-ZIFs was because PMS was an unstable chemical and can self-decompose, self-producing $\cdot\text{OH}$ radicals and $\text{SO}_4^{\cdot-}$ sulfate radicals in very small amounts, and the small amount of RhB concentration. However, when adding $0.05 \text{ g}\cdot\text{L}^{-1}$ of CuZn-ZIFs material to the reaction system, the efficiency reached 43%, an increase of more than 30% compared to without a catalyst, and continued to increase to 76.2% at 0.1 mg and 99.1% at $0.15 \text{ g}\cdot\text{L}^{-1}$ with a difference of about 20 - 30% for each dose, but when increasing the dose from $0.2\text{--}0.25 \text{ g}\cdot\text{L}^{-1}$ the effectiveness reached a maximum of 100%. This has proven the important role of CuZn-ZIFs catalyst in decomposing RhB. The higher the amount of CuZn-ZIFs, the more Zn^{2+} and Cu^{2+} metal centers, the faster the reaction occurs, so the removal efficiency was higher. However, with its non-selective and strong activity characteristics, $\cdot\text{OH}$ radicals produced in excess would easily attack each other and attack PMS, reducing the amount of $\cdot\text{OH}$ available, as well as using too much, amount of catalyst leads to waste of raw materials throughout the process. That was also the reason why, when continuing to increase the catalyst mass, the RhB removal efficiency tended to balance. Therefore, the use of excess catalyst was not necessary and the optimal CuZn-ZIFs catalyst dosage was chosen to be $0.15 \text{ g}\cdot\text{L}^{-1}$.

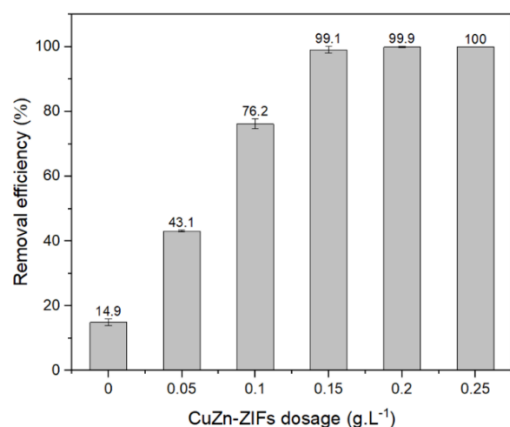


Figure 5. RhB removal efficiency of CuZn-ZIFs/PMS system with different CuZn-ZIFs dosage

Experimental conditions: RhB concentration of $40 \text{ mg}\cdot\text{L}^{-1}$, pH = 4, CuZn-ZIFs:PMS ratio (1:4), room temperature and reaction time of 60 min.

3.2.4. Influence of PMS dosage

In this study, PMS is the main agent involved in the degradation of RhB thanks to its ability to decompose and generate hydroxyl radical. As the above experiment shows, under normal conditions, without irradiation or catalyst, PMS still has the ability to decompose to create $\cdot\text{OH}$ but at a very slow rate and at a very low dose, leading to low treatment efficiency. In theory, the more PMS used, the more free radicals are generated, thereby bringing about higher waste treatment efficiency. To verify that, the influence of PMS on RhB degradation efficiency was investigated. Specifically, to perform the experiment, the factors surveyed and selected include the initial concentration of RhB of $40 \text{ mg}\cdot\text{L}^{-1}$ with pH 4, and the amount of CuZn-ZIFs material is $0.15 \text{ g}\cdot\text{L}^{-1}$. The amount of PMS used corresponds to the amount of material in the ratio 1:1, 1:2, 1:3, 1:4, and 1:5. The reaction was performed at room temperature for 60 minutes. The results are presented in Figure 6.

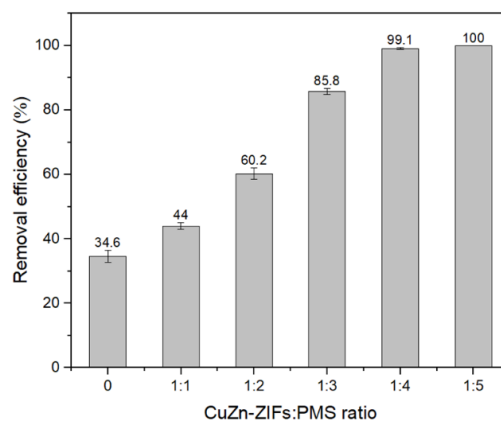


Figure 6. RhB removal efficiency of CuZn-ZIFs/PMS system with different CuZn-ZIFs:PMS ratio

Experimental conditions: RhB concentration of $40 \text{ mg}\cdot\text{L}^{-1}$, CuZn-ZIFs dosage of $0.15 \text{ g}\cdot\text{L}^{-1}$, pH = 4, room temperature and reaction time of 60 min.

The results showed that the amount of PMS had an effect on RhB degradation, with a similar trend to the catalyst. When only CuZn-ZIFs and RhB catalysts are present, the removal efficiency is very low, about 35%. With the weight ratio of CuZn-ZIFs:PMS increasing from 1:1 to 1:2 and 1:3, the RhB attenuation increased from 44% to 60.2% and 85.8% difference, respectively. Gradually increase the effectiveness when increasing the amount of PMS by about 20%. At higher ratios, 1:4 and 1:5,

the removal efficiency did not change much and remained constant at 99.1 - 100%. Compared to the sample with only RhB catalyst, the mechanism of the treatment process is mainly adsorption because the CuZn-ZIFs material has a porous structure. When using PMS, the decomposition of PMS is activated by the CuZn-ZIFs heterogeneous catalyst due to the two catalytic centers Cu^{2+} and Zn^{2+} , leading to the generation of $\cdot\text{OH}$ radical and sulfate radical $\text{SO}_4^{\cdot-}$, which mainly contribute to the dye decomposition. As can be seen at a ratio of CuZn-ZIFs:PMS of 1:4, the process of dye decomposition begins to reach equilibrium; thus the optimal ratio of CuZn-ZIFs:PMS was selected at 1:4.

3.2.5. Influence of temperature

In a chemical reaction, temperature greatly affects the reaction process. Therefore, the temperature was investigated at room temperature levels, 40°C, 50°C and 60°C. To experiment, the factors were investigated and selected in the previous experiment, including the initial concentration of RhB of $40 \text{ mg}\cdot\text{L}^{-1}$ with pH 4, and the volume of CuZn-ZIFs material is $0.15 \text{ g}\cdot\text{L}^{-1}$. The ratio between catalyst and PMS is 1:4, and the reaction is carried out in 60 minutes at different temperature conditions. The results are presented in Figure 7.

Based on the results of RhB decomposition according to temperature, it shows that the more the temperature increases, the more effective the decomposition efficiency is. When increasing from room temperature to 40°C, the treatment efficiency difference is not too much, only from 99.1 to 99.8% of the difference. 0.7%, continuing to increase the temperature from 50°C and 60°C, the treatment efficiency reaches a maximum of 100%. In the RhB catalytic decomposition reaction, essentially two main processes will occur, the first is the CuZn-ZIFs process that catalyzes the decomposition of PMS to create $\cdot\text{OH}$ radical and $\text{SO}_4^{\cdot-}$ sulfate radical, and the second is the process by which the $\cdot\text{OH}$ radical and the sulfate radical $\text{SO}_4^{\cdot-}$ are produced decompose RhB. When the temperature increases, this factor will affect both processes simultaneously. In principle, increasing temperature will increase the reaction rate in most reactions and this is true in the above survey. This can be explained based on the mechanism as well as the properties of the oxidizing agent (free radical $\cdot\text{OH}$). During the first 30 minutes, high temperatures will help stimulate the production of many free radicals, so the RhB decomposition rate is therefore higher than low temperatures. This characteristic is only beneficial in a certain short

time, but is detrimental in the long term, because the $\cdot\text{OH}$ free radical is a strong oxidizing agent and is not selective, creating too many free radicals. $\cdot\text{OH}$ in a short time, in addition to attacking the dye molecules, also attacks itself and PMS, thereby leading to the loss of oxidizing agents, causing waste throughout the processing process. At room temperature, the decomposition rate is stable compared to all temperature levels and can be stopped at 60 minutes with 99% efficiency. Therefore, room temperature is considered the best choice in this study.

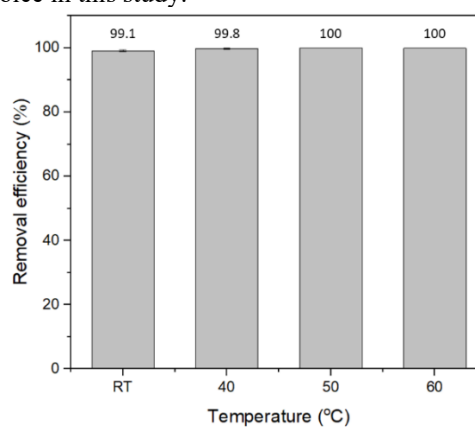


Figure 7. RhB removal efficiency of CuZn-ZIFs/PMS system with different reaction temperatures

Experimental conditions: RhB concentration of $40 \text{ mg}\cdot\text{L}^{-1}$, CuZn-ZIFs dosage of $0.15 \text{ g}\cdot\text{L}^{-1}$, CuZn-ZIFs:PMS ratio (1:4), pH = 4 and reaction time of 60 min.

3.2.6. Influence of reaction time

The next factor chosen for further investigation is the effect of time on RhB decomposition efficiency. The reaction was carried out under the optimal conditions investigated in the above experiments at room temperature, the mass of CuZn-ZIFs was $0.15 \text{ g}\cdot\text{L}^{-1}$, the ratio between catalyst and PMS was 1:4 and the initial RhB concentration was $40 \text{ mg}\cdot\text{L}^{-1}$ with pH 4. The reaction is performed at different time points from 10 to 60 minutes. The results are presented in Figure 8. Experiments demonstrate that longer reaction times lead to increased RhB decomposition efficiency. In the first 10 minutes, efficiency reached 27.18%, when increasing the time increased from 10 minutes to 20 minutes, efficiency reached 45.6%. Continue to increase the time from 30 to 40 minutes, and the efficiency gradually increases from 55.6% to 76.1%, the difference when gradually increasing the time is about 10 - 20%, and after 50 and 60 minutes the

efficiency reaches more than 99%. The reason is that the longer the time, the higher the ability of CuZn-ZIFs to catalyze PMS to produce hydroxyl radicals and create more conditions for RhB to be decomposed. Besides, the molecular structure of RhB is quite complex, containing many aromatic rings and stable double bonds, so to be able to decompose thoroughly as well as increase the efficiency of the whole process, a long time is a factor necessary element. Although at 60 minutes, the RhB removal efficiency was very consistent at about 99%, this efficiency did not differ too much from that at 50 minutes. Maintaining an additional 10 minutes of reaction without much difference in performance is not economically meaningful. Therefore, the reaction time of 50 minutes is the optimal level chosen for this survey.

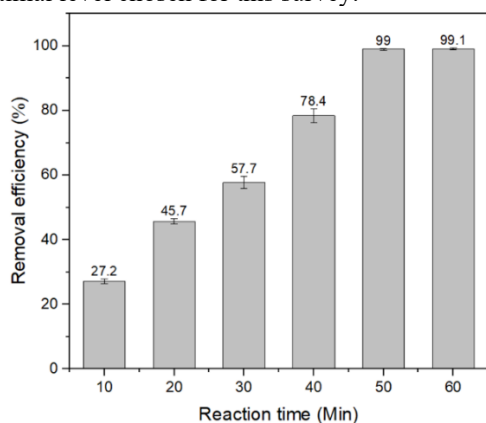


Figure 8. RhB removal efficiency of CuZn-ZIFs/PMS system with different reaction time: RhB concentration of 40 mg·L⁻¹, CuZn-ZIFs dosage of 0.15 g·L⁻¹, CuZn-ZIFs: PMS ratio (1:4), room temperature and pH = 4.

3.2.7. Influence of different oxidizers

To assess the degradation efficiency of RhB, three oxidizing agents were employed: PMS, H₂O₂, and O₂. With experimental conditions included catalyst dosage used was 0.15 g·L⁻¹, corresponding to the amount of PMS used in a ratio of 1:4, room temperature, a reaction time of 50 minutes, RhB concentration of 40 mg·L⁻¹, and pH 4. The experiment was performed three times to provide average results, and the results are presented in Figure 9 which shows that the efficiency of RhB degradation varied significantly depending on the oxidizing agent. H₂O₂ and O₂ had negligible degradation effect due to their low oxidizing capacity producing minimal hydroxyl ·OH radicals, resulting in a low degradation efficiency of 35-40%, PMS, being a strong oxidizing agent,

generated a high concentration of ·OH and sulfate radicals SO₄^{·-}, effectively degrading RhB with an efficiency of up to 99%. These results highlight the superior performance of PMS as an oxidizing agent for RhB removal, attributed to its ability to generate a high quantity of free radicals that decompose the dye effectively.

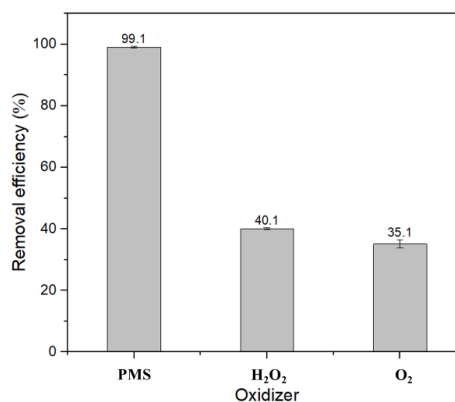


Figure 9. RhB removal efficiency of CuZn-ZIFs/PMS system with a different oxidizer
Experimental

conditions: RhB concentration of 40 mg·L⁻¹, CuZn-ZIFs dosage of 0.15 g·L⁻¹, CuZn-ZIFs:PMS ratio (1:4), pH = 4, room temperature and reaction time of 50 min.

3.3. Reusability of CuZn-ZIFs

3.3.1. Investigate the reuse ability of CuZn-ZIF through each cycle

CuZn-ZIFs was evaluated for recovery and reuse, implementation conditions were based on the optimal levels of each of the above survey factors, including the CuZn-ZIFs dosage was 0.15 g·L⁻¹ corresponding to the amount of PMS used in a ratio of 1:4, room temperature, time of 50 minutes, RhB concentration of 40 mg·L⁻¹, and pH 4. The experiment was performed three times to provide average results. The results showed that CuZn-ZIFs still had good activity after several reuses (Figure 10). It was worth noting that the catalytic degradation of RhB reached 99.1% in the first cycle, and the second time, the efficiency reached 98.7%. Continue to reuse, the efficiency reaches 98.5% in the third cycle. However, the 4th and 5th times the efficiency was 95.8% and 90.8%, respectively. From the above results, we see that the material ensured high treatment efficiency after 5 reuses, with efficiency reaching over 90%. Hence, it could be confirmed that CuZn-ZIFs possessed the reusability for RhB degradation.

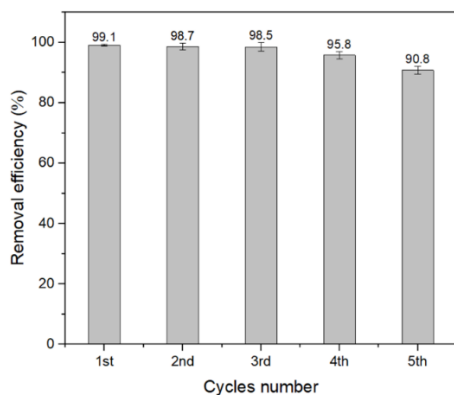


Figure 10. RhB removal efficiency of CuZn-ZIFs/PMS system during recovery and reuse process

Experimental conditions: RhB concentration of 40 mg·L⁻¹, CuZn-ZIFs dosage of 0.15 g·L⁻¹, CuZn-ZIFs:PMS ratio (1:4), pH = 4, room temperature and reaction time of 50 min.

3.3.2. Characteristics of the reused CuZn-ZIFs

The recovered CuZn-ZIFs were subjected to a continuous methanol wash for a duration of five days. This extensive process was carried out to confirm the complete removal of post-treatment intermediates and residual RhB. Subsequently, the CuZn-ZIFs underwent comprehensive examination

of their structural, bonding, and functional group properties using FT-IR and PXRD techniques. The results of these analyses are illustrated in Fig. 11.

Figure 11 (a) illustrates that the FT-IR spectra revealed the peaks persisted at the same distinctive positions as the fresh material, despite a slight shift that had minimal impact on the material's structure. However, the intensity of the peak for the reclaimed material was significantly lower than the reused material. To be specific, the vibration of the metal-N bond at 420 cm⁻¹ (fresh) to 421 cm⁻¹ (reused), and the imidazolate ring vibrations from 600 cm⁻¹ to 2000 cm⁻¹ remained consistent but decreased in intensity due to loss after repeated recycling. The position of the C=N bond in the infrared spectrum of CuZn-ZIFs (fresh) shifted from 1586 cm⁻¹ to 1583 cm⁻¹ (reused) or 1423 cm⁻¹ (fresh) to 1422 cm⁻¹ (reused). Besides, the position of the C-H bond in the infrared spectrum of CuZn-ZIFs (fresh) shifted from 1147 cm⁻¹, 995 cm⁻¹, 760 cm⁻¹ to 1146 cm⁻¹, 994 cm⁻¹, 756 cm⁻¹ (reused). The material's characteristic bond positions did not exhibit drastic changes. Thus, it is highly probable that the CuZn-ZIFs maintained their initial structure. Nevertheless, the outcomes derived from the FT-IR technique were inconclusive in determining whether the material's crystalline structure remained intact.

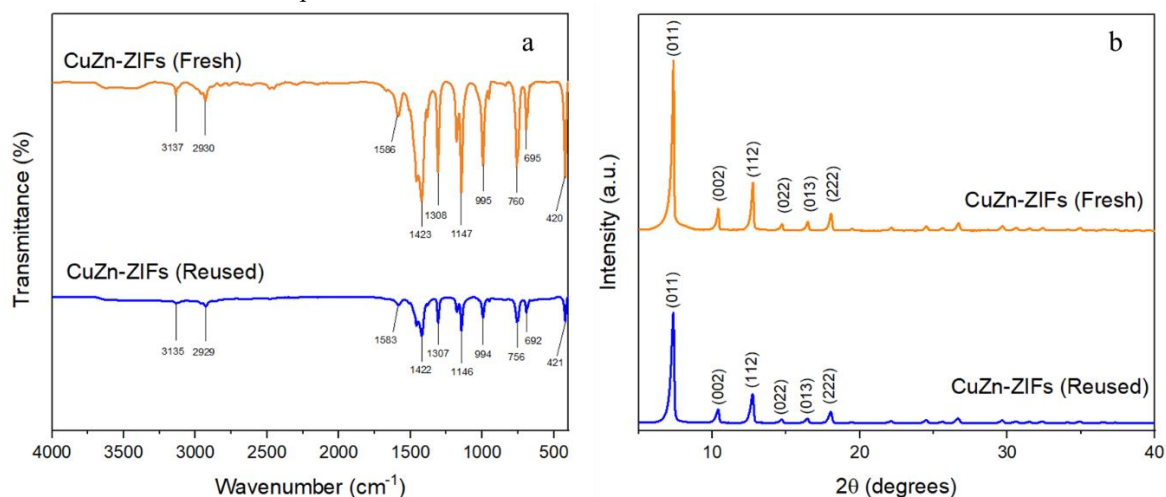


Figure 11. FT-IR spectra (a) and PXRD (b) pattern of CuZn-ZIFs fresh and CuZn-ZIFs reused

Figure 11 (b) illustrates that the retrieved material underwent additional examination through the PXRD technique. The findings indicated that the PXRD profile of the reused CuZn-ZIFs closely resembled the PXRD profile of the fresh CuZn-ZIFs. Specifically, the positions associated with the planes (011), (002), (112), (022), (013), (222)

persisted in the CuZn-ZIFs form following recovery and reuse. Consequently, the catalyst maintained its structure and activity after being utilized five times to catalyze the breakdown of RhB.

4. CONCLUSION

In summary, CuZn-ZIFs material has been successfully synthesized by the solvothermal method combined with ultrasonic cleaned under relatively mild conditions, without the assistance of pressure with a material synthesis efficiency of over 50% and extensively characterized using various analytical techniques. This material was employed as an effective heterogeneous catalyst for RhB degradation in an aqueous solution with the addition of PMS. The results showed that RhB dye degradation efficiency achieved over 99% within 50 minutes under optimal conditions. In detail, it occurred in the presence of a 20 mL RhB solution with an initial concentration of 40 mg.L⁻¹ at pH 4, 0.15 g·L⁻¹ catalyst dosage with the dosage ratio of the catalyst CuZn-ZIFs: PMS was 1:4 at room

temperature. Additionally, CuZn-ZIFs could be regenerated and reused four times while exhibiting higher catalytic activity than other homogeneous and heterogeneous catalysts. A newly developed catalyst called bimetallic CuZn-ZIFs has shown remarkable potential in treating toxic textile waste with high efficiency. This breakthrough could contribute significantly to environmental protection efforts by reducing the harmful impact of textile waste on the planet.

ACKNOWLEDGMENT

This work was supported by B2023-TCT-22 project funding from the Ministry of Education and Training, Viet Nam. The authors thank Faculty of Chemical Engineering of Can Tho University for the facilities and analysis.

REFERENCES

- Asad, S., Amoozegar, M. A., Pourbabae, A. A., Sarbolouki, M. N., & Dastgheib, S. M. M. (2009). Decolorization of textile azo dyes by newly isolated halophilic and halotolerant bacteria. *Bioresource Technology*, 98(11), 2082-2088. <https://doi.org/10.1016/j.biortech.2006.08.020>
- Assfour, B., Leoni, S., Seifert, G., & Baburin, I. A. (2011). Packings of carbon nanotubes—new materials for hydrogen storage. *Advanced Materials*, 23(10), 1237-1241. <https://doi.org/10.1002/adma.201003669>.
- Awadallah, S., Hasan, H., Attlee, A., Raigangar, V., Unnikannan, H., Madkour, M., Abraham, M. S. & Rashid, L. (2019). Waist circumference is a major determinant of oxidative stress in subjects with and without metabolic syndrome. *Diabetes & Metabolic Syndrome: Clinical Research & Reviews*, 13(4), 2541-2547. <https://doi.org/10.1016/j.dsx.2019.07.010>.
- Budi, C. S., Deka, J. R., Hsu, W. C., Saikia, D., Chen, K. T., Kao, H. M., & Yang, Y. C. (2021). Bimetallic Co/Zn zeolitic imidazolate framework ZIF-67 supported Cu nanoparticles: An excellent catalyst for reduction of synthetic dyes and nitroarenes. *Journal of Hazardous Materials*, 407, 124392. <https://doi.org/10.1016/j.jhazmat.2020.124392>.
- Carmen, Z., & Daniela, S. (2012). *Textile organic dyes-characteristics, polluting effects and separation/elimination procedures from industrial effluents-a critical overview* (Vol. 3). IntechOpen Rijeka. DOI: 10.5772/32373.
- Chandanshive, V., Kadam, S., Rane, N., Jeon, B. H., Jadhav, J., & Govindwar, S. (2020). In situ textile wastewater treatment in high rate transpiration system furrows planted with aquatic macrophytes and floating phytobeds. *Chemosphere*, 252, 126513. <https://doi.org/10.1016/j.chemosphere.2020.126513>.
- Dai, M., Wang, Z., Wang, F., Qiu, Y., Zhang, J., Xu, C. Y., Zhai, T., Cao, W., Fu, Y., Jia, D., Zhou, Y., & Hu, P. A. (2019). Two-dimensional van der Waals materials with aligned in-plane polarization and large piezoelectric effect for self-powered piezoelectric sensors. *Nano Letters*, 19(8), 5410-5416. <https://doi.org/10.1021/acs.nanolett.9b01907>.
- Dey, M., Mann, B. R., Anshu, A., & Mannan, M. A. (2014). Activation of protein kinase PKR requires dimerization-induced cis-phosphorylation within the activation loop. *Journal of Biological Chemistry*, 289(9), 5747-5757. <https://doi.org/10.1074/jbc.M113.527796>.
- Fatima, A., & Sultana, H. (2009). Tracing out the U-shape relationship between female labor force participation rate and economic development for Pakistan. *International Journal of Social Economics*, 36(1/2), 182-198. <https://doi.org/10.1108/03068290910921253>.
- Lachheb, H., Puzenat, E., Hounas, A., Ksibi, M., Elaloui, E., Guillard, C., & Herrmann, J. M. (2002). Photocatalytic degradation of various types of dyes (Alizarin S, Crocein Orange G, Methyl Red, Congo Red, Methylene Blue) in water by UV-irradiated titania. *Applied Catalysis B: Environmental*, 39(1), 75-90. [https://doi.org/10.1016/S0926-3373\(02\)00078-4](https://doi.org/10.1016/S0926-3373(02)00078-4).
- Lee, H. S., Barton, S. J., & Rebec, G. V. (2012). Neural correlates of unpredictability in behavioral patterns of wild-type and R6/2 mice. *Communicative & Integrative Biology*, 5.
- Li, H., Yin, S., Wang, Y., & Sato, T. (2013). Efficient persistent photocatalytic decomposition of nitrogen monoxide over a fluorescence-assisted CaAl₂O₄:(Eu,

- Nd)/(Ta, N)-codoped TiO₂/Fe₂O₃. *Applied Catalysis B: Environmental*, 132, 487-492. <https://doi.org/10.1016/j.apcatb.2012.12.026>.
- Kumar, M., Kaur, P., Garg, R., Patil, R. K., & Patil, H. C. (2020). A study on antibacterial property of curcuma longa – herbal and traditional medicine. *Journal of Medical Sciences & Research*, 2(2), 103-108. https://doi.org/10.25259/AUJMSR_11_2020.
- Nagarjun, N., & Dhakshinamoorthy, A. (2019). Liquid phase aerobic oxidation of cyclic and linear hydrocarbons using iron metal organic frameworks as solid heterogeneous catalyst. *Molecular Catalysis*, 463, 54-60. <https://doi.org/10.1016/j.mcat.2018.11.012>.
- Ren, Q., Nie, M., Yang, L., Wei, F., Ding, B., Chen, H., Liu, Z., & Liang, Z. (2022). Synthesis of MOFs for RhB adsorption from wastewater. *Inorganics*, 10(3), 27. <https://doi.org/10.3390/inorganics10030027>.
- Samuel, M. S., Savunthari, K. V., & Ethiraj, S. (2021). Synthesis of a copper (II) metal-organic framework for photocatalytic degradation of rhodamine B dye in water. *Environmental Science and Pollution Research*, 28(30), 40835-40843. <https://doi.org/10.1007/s11356-021-13571-9>.
- Schejn, A., Aboulaich, A., Balan, L., Falk, V., Lalevée, J., Medijahdi, G., Aranda, L., Mozet, K., & Schneider, R. (2015). Cu²⁺ doped zeolitic imidazolate frameworks (ZIF-8): efficient and stable catalysts for cycloadditions and condensation reactions. *Catalyst Science Technology*, 5, 1829-1839.
- Song, Y., Wang, K., Zhao, F., Du, Z., Zhong, B., & An, G. (2022). Preparation of powdered activated carbon composite material and its adsorption performance and mechanisms for removing RhB. *Water*, 14(19), 3048. <https://doi.org/10.3390/w14193048>.
- Wang, Y., Zhang, X., Zhang, H., Lu, Y., Huang, H., Dong, X., Chen, J., Yang, X., Hang, H., & Jiang, T. (2012). Coiled-coil networking shapes cell molecular machinery. *Molecular Biology of the Cell*, 23(19), 3911-3922. <https://doi.org/10.1091/mbc.E12-05-0396>.
- Wang, S., & Zhu, Z. H. (2007). Effects of acidic treatment of activated carbons on dye adsorption. *Dyes and Pigments*, 75(2), 306-314. <https://doi.org/10.1016/j.dyepig.2006.06.005>.
- You, L., Huang, C., Lu, F., Wang, A., Liu, X., & Zhang, Q. (2018). acile synthesis of high performance porous magnetic chitosan-polyethylenimine polymer composite for Congo red removal. *International Journal of Biological Macromolecules*, 107, 1620-1628. <https://doi.org/10.1016/j.ijbiomac.2017.10.025>.
- Yusuf, A., Wright, N., Steiman, M., Gonzalez, M., Karpur, A., Shih, A., Shikako, K., & Elsabbagh, M. (2022). Factors associated with resilience among children and youths with disability during the COVID-19 pandemic. *PLOS ONE*, 17, 7. <https://doi.org/10.1371/journal.pone.0271229>.
- Zhang, J., & Liu, K. (2020). Enhanced Adsorption of Doxycycline Hydrochloride (DCH) from Water on Zeolitic Imidazolate Framework-8 Modified by Cu²⁺ (Cu-ZIF-8). *Water Air and Soil Pollution*, 231, 91. <https://doi.org/10.1007/s11270-020-4455-8>.
- Zhong, J., Sun, Y., Peng, W., Xie, M., Yang, J., & Tang, X. (2018). An XGBoost-based framework for essential protein prediction. *IEEE Trans Nanobioscience*, 17(3), 243-250. <https://doi.org/10.1109/TNB.2018.2842219>.